INTRODUCTION

INTRODUCTION

1. Surfactant and its aggregation.

Surfactants, generally organic compounds, are amphiphilic in nature, comprise hydrophilic head group and hydrocarbon tail, exhibiting dual affinity to water and oil. Its amphiphilicity promotes its adsorption at air-liquid and /or liquid-liquid (otherwise immiscible) interface, besides its capability to lower interfacial tension (γ). Soaps, detergents, long chain alcohols and lipids are amphiphilic in nature and can effectively reduce interfacial tension.[1] Besides its chemical structure, interfacial and aggregation behavior of surfactants depend on environmental conditions like temperature, pressure, solvent and additives.[2-5] Formation of associated colloid is one of the most important properties of amphiphiles by its self aggregation. Self-aggregation behavior of amphiphiles in polar solvent was first proposed by McBain.[6] SURface ACTive AgeNT or 'SURFACTANT' is one of the important components in biological systems, drug delivery,[7] gene therapy,[8] DNA transfection,[9] and nanoparticle synthesis.[10] That can improve quality in every part of life, *viz.* cosmetic,[11] food,[12] medicine,[13] toothpaste,[14] textile[15] and detergents.[16] In polar protic solvents, surfactants prefer to adsorb at air-liquid interface where the non-polar part protrudes away from the solvent while the head groups of hydrophilic part are oriented towards the solvent; such an orientation is induced by hydrophilic head group-solvent interaction, schematically shown in Figure 1. Adsorption of surfactants molecules from the bulk to air-water interface involves two steps: (i) movement of the surfactant molecules from the bulk to sub-surface and (ii) motion of the surfactants molecules from the sub-surface to air-water interface. After complete interfacial adsorption, the surface becomes saturated forcing the surfactants to congregate into sphere like entities called micelles, where the hydrophilic head groups are oriented outward, protecting the hydrocarbon chain from the polar solvents. In case of nonpolar solvents, reverse micelles are formed whereby the orientation of the surfactant in the aggregates are opposite.

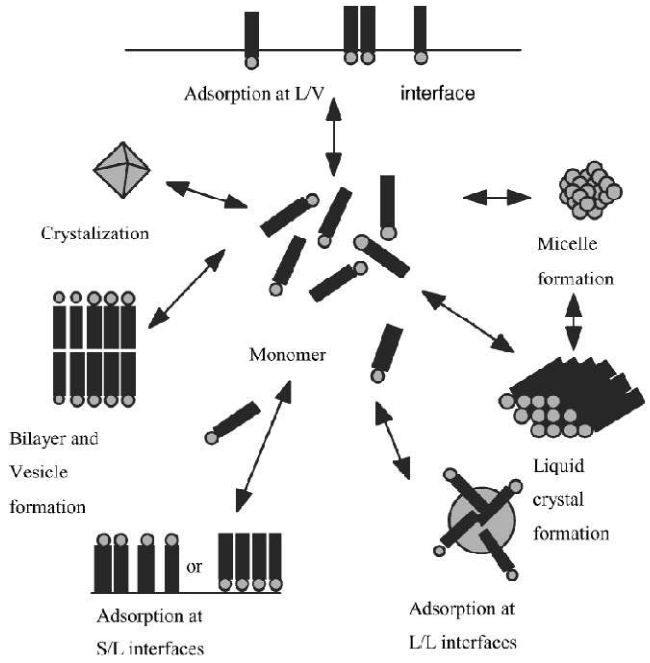

Figure 1. Packing parameter and related shapes of aggregates. Adopted from Myers et al.[17]

2. Classification of surfactants

2.1. Based on origin.

2.1.1. Soap. Soaps, the natural surfactants, are produced by the alkaline hydrolysis of fats; the chemical reaction is called safonification.[18-20] They are less soluble in hard water but are fairly soluble in soft water. Some examples of soaps are sodium palmitate, sodium stearate and sodium oleate.

2.1.2. Detergent. Synthetically prepared surfactants are known as detergents.[21] Detergents can withstand hard water unlike soap molecules as the polar moieties of surfactants interact weakly with the components of hard water. Some examples of detergents are sodium dodecylbenzensulphonate, sodium dodecylsulphate, hexadecyltrimethylammonium bromide, hexadecylpyridinium chloride and polyoxyethylenesorbitan monolaurate, *etc*.

2.2. *Based on the charge carried by the hydrophilic moiety.*

2.2.1. Anionic Surfactant. Anionic surfactants are dissociated in water molecules and form amphiphilic anions and counter cations like alkali metals. Alkylbenzene sulphonate (detergents), sodium or potassium salt of fatty acids (soaps), lauryl sulphate (foaming agents), di-alkyl sulfosuccinates (wetting agents) and lignosurfactants (dispersants) are some of the examples of

anionic surfactants. In dicarboxylic *N*-dodecylamino acid based surfactants (C_{12}AAS)Na_2, two carboxylate groups are solvated by water and the dodecyl chains get oriented into the core of micelles. The carboxylate groups of *N*-dodecylaminomalonate, *N*-dodecylaminoaspartate and *N*-dodecylaminoglutamate are separated by one, two and three methylene group(s) while the amide bond connects the hydrophobic tail to the polar head group. (C_{12}AAS)Na_2 can have potential applications in different fields, *viz.*, biochemical research,[22] as detergents, surfactant-based separation,[23] surface wetting modification, flotation,[24] and for the synthesis of a variety of catanionic and zwitterionic surfactants.[25]

2.2.2. Cationic Surfactant. Cationic surfactants spontaneously dissociate in water to form amphiphilic cations with usually the halides as the counter anions. Long chain alkyltrimethylammonium halides, benzalkonium halide, benzethonium halides and long chain alkylpyridinium halides are some examples of cationic surfactants.

2.2.3. Nonionic Surfactant. Nonionic surfactants, do not have ionisable moities and hence they do not dissociate into ions in aqueous medium. Examples include sorbitan monolaurate (Span 20) and polyoxyethylene sorbitan monolaurate (Tween 20), *etc*.

2.2.4. Zwitterionic Surfactant. Zwitterionic surfactants contain both the cations and anions groups. 1,2-diacyl-sn-glycore-3-phosphatidylcholine (lecithin), 3- (ethyldimethylammonio) propane - 1- sulfonate (NDSB-195), soy phosphatidylcholine (SPC) and hydrogenated soy phosphatidylcholine (HSPC) are some of the examples of zwitterionic surfactants.

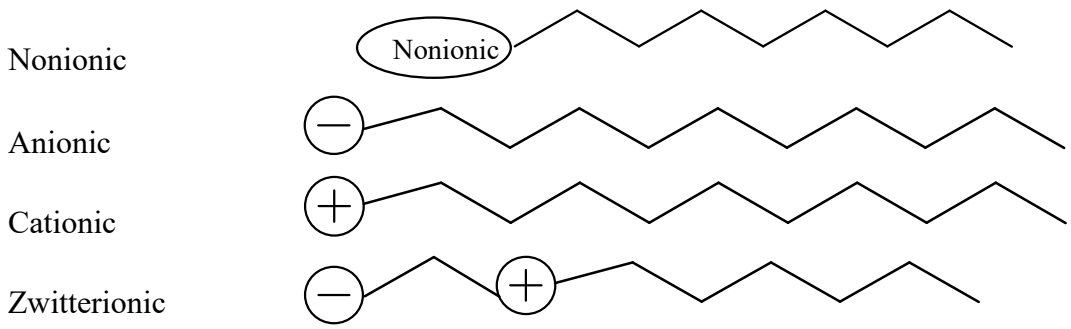

Figure 2. Surfactant classification according to the composition of head groups: non-ionic, anionic, cationic and zwitterionic. Adopted from Schramm et al.[26]

2.2.5. Metallosurfactants. Ionic surfactants interact with oppositely charged mononvalent, bivalent and trivalent ions to form stable complexes, act as chelating agents, shown in Scheme 1.

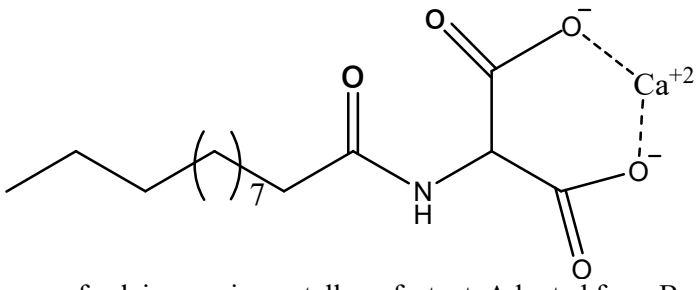

Scheme 1. Schematic diagram of calcium aminometallosurfactant. Adopted from Bordes et al.[25]

Bivalent metals electrostatically interact with anionic surfactants to form chelate metal complexes, known as metallosurfactants.[27] They can form micelle, vesicle as well as soluble or insoluble monolayers at air-water interface.[28,29] Examples of metallosurfactants are calcium *N*-dodecylaminomalonate and calcium *N*-tetradecylaminoaspartate, bis hexadecyl pyridinium iron (FeCPC II) tetrachloride and bishexadecyl pyridinium cobalt (CoCPC II) tetrachloride, *etc.*[29]

2.3. Other classifications.

New classes of surfactants have emerged with different structures and bonding by virtue of the developments of surface chemistry. These include the gemini surfactants, bolaamphiphiles and catanionic surfactants.

2.3.1. Gemini surfactant. In gemini surfactants, hydrophilic moieties or the adjoining hydrocarbon segments of two conservative surfactant molecules are closely linked through covalent bond.[30-33] The terminal hydrocarbon chains may be short or long; however the two polar head groups could be either cationic, anionic or non-ionic in nature. Spacers between the two head groups are short or long, flexible or rigid.[34, 35] Hydrocarbon chain attach between two identical head groups, (Figure 3). Two head groups are separated by 3-4 methylene moieties.[36-38]

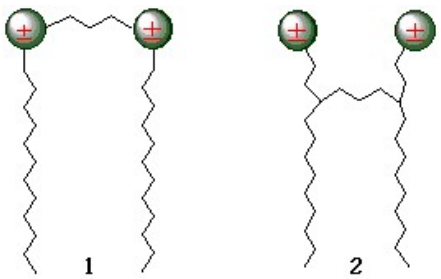

Figure 3. Schematic representation of two types of gemini surfactants. Adopted from Du et al.[35]

2.3.2. Bolaamphiphile. In bolaform surfactants, also known as bolaamphiphiles, two hydrophilic head groups are attached at both end of a hydrophobic chain.[39, 40]

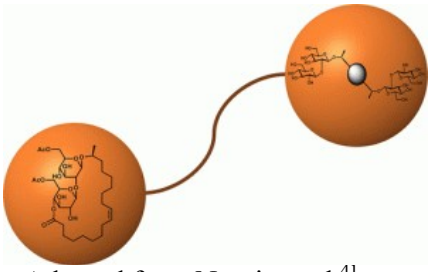

Figure 4. Structure of bolaamphiphile. Adopted from Nuraje et al.[41]

2.3.3. Catanionic Surfactant. When oppositely charged surfactants are stoichimetrically mixed in aqueous medium, charge neutralisation of the head groups leads to the formation of insoluble precipitate. The coacervates, also known as ion pair amphiphiles or catanionic surfactants can be considered as pseudo double tailed (generally, or higher in case of surfactants having more than one hydrocarbon chain) entities can be considered as substitutes of natural phospholipids in formulating synthetic hybrid vesicles. Schematic structure of catanioinic surfactant has been shown in Figure 5.

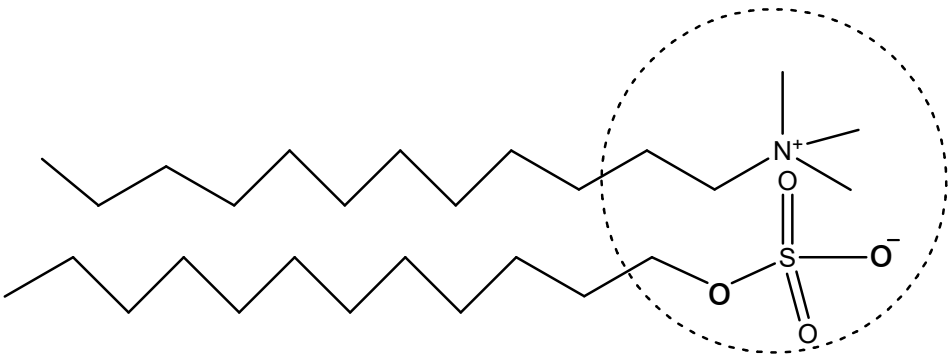

Figure 5. Molecular structure of catanionic surfactant that can be formed by the interaction between dodecyltrimethylammonium bromide and sodium dodecylsulphate.

Catanionic surfactants exhibit unique characteristics, differ substantially from the individual precursors, that include i) lower critical micelle concentration (*CMC*) than the individual component, ii) higher surface activity and iii) capability to form various aggregates, *viz.*, spherical micelles, vesicles and planar bilayer.[42] Unique properties of catanionic surfactants are due to the strong synergistic interaction between the constituent surfactants.[43-48]

3. Interfacial and bulk properties of surfactants.

In presence of polar protic solvents, surfactant molecules adsorb at air-liquid interface that reduce the interaction between the hydrophobic tails with the polar solvent as schematically shown in Figure 6. Non polar part of surfactant molecules are protruded away from the solvent at air-water interface. While the hydrophobic repulsion favours the congregation of surfactants after a certain concentration is reached (known as critical micelle concentration, *CMC*), hydrophilic head groups (more prominent in case of ionic surfactants) retard the self-aggregation process.[49]

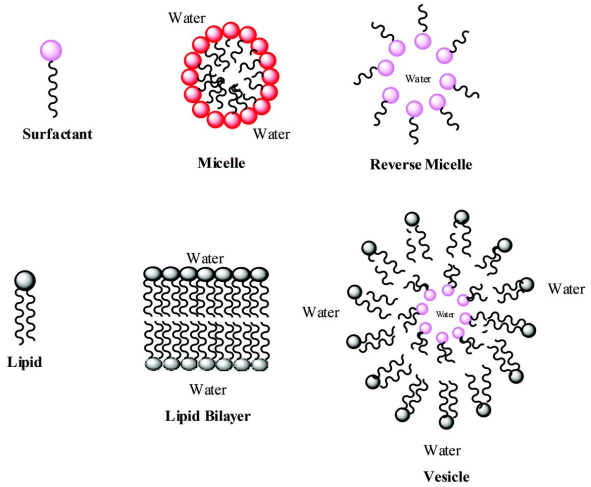

Figure 6. Schematic orientation and aggregation of surfactant molecules in polar solvents. Adopted from Warnheim et al.[50]

Apparently it may be assumed that the processes of micellization, which results in the formation of organized assemblies, may be nonspontaneous processes. However the process of micellization is a spontaneous one where the over all negative free energy change originates from the larger positive entropy change, whereby micellization process is entropy dependent.[51] When dissolution of surfactant occurs, hydrophobic group changes the hydrogen bonding structure of water, increases free energy in the system. Higher micellar surface charge density and fraction of counter ion binding are the dominant factors in reducing the repulsive forces between polar head groups of ionic surfactant.[49]

4. Critical packing parameter.

Various self assembly form of surfactants depend the nature and geometry of amphifiles. Critical packing parameter values can be evaluated using the Israelachvili's proposition:[52]

$$P = \frac{v}{Al_c} \quad (1)$$

$$R^{\mathrm{M}} = \frac{3\mathrm{v}}{A} \quad (2)$$

where, P, l_c and v values denote packing parameter, length and volume of the hydrophobic chain, respectively. R^{M} and A indicate the radius of micelle and cross sectional area of surfactant head group, respectively. The corresponding volumes (v) can be defined using Tanford's formula:[52]

$$l_c \leq l_{max} \approx (0.154+0.1265\ \mathrm{n}) \quad (3)$$

and

$$v = (0.0274+0.0269) \quad (4)$$

where, l_{max} is maximum length of the hydrophobic chain. Shape of aggregates can be defined by the packing parameter of surfactant mixtures using appropriate propositions.

5. **Surfactant aggregation in solution.** Depending on the polarity of solvent, different types of aggregates are formed by surfactant molecules.

5.1. Micelle. Micelles are formed in polar solvents where the hydrophilic head groups are fascinated to water and non-polar moities are delineated away from water. Various types of aggregates including spherical,[54] disc like,[54] lamellar,[55] and spheroidal,[43] micelles are formed, which schematically shown in (Figure 7).

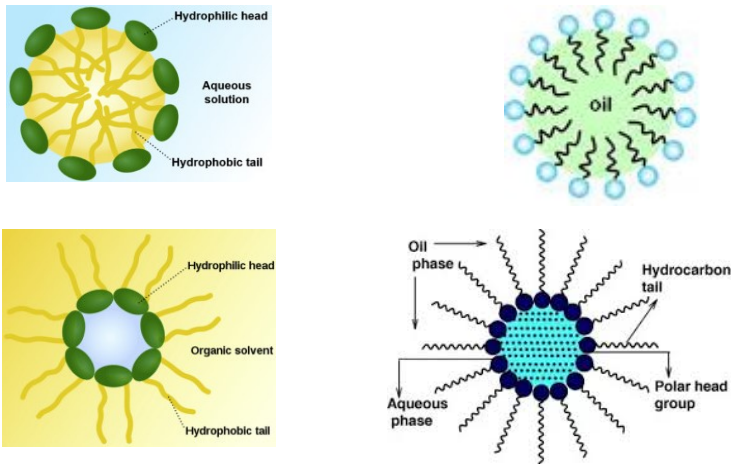

Figure 7. Schematic representation for micelle, oil-in-water micelle, reverse, and water-in-oil reverse micelles.Adopted from Harkins et al.[54]

5.2. Reverse micelle. Reverse micelles are formed in nonpolar medium. In case of reverse micelles, the orientations of the surfactants are opposite to the micelles formed in polar solvents. The head groups are oriented inward with the hydrocarbon moieties remain solubilised in the nonpolar solvent. Micelles and reverse micelles are capable of accommodating oil and water respectively and hence microemulsions are formed. Thus a nonpolar solvent can be dispersed in a polar solvent and vice versa with the aid of surfactants.

5.3. Microemulsion. Microemulsions are thermodynamically stable, usually clear and isotropic dispersions of water in oil or vice versa stabilized by surfactant monolayer. Some times small chain alkanols, alkyl amines are necessary to be used along with surfactants in forming stable microemulsions. These short chain species are known as co-surfactants. Oil-in-water microemulsions are considered as oil-swollen micelles, while the water-in-oil microemulsion is called water-swollen reverse micelles (Figure 7).

The presence of counterion significantly reduces the repulsion between the surfactant head groups. The counter ions situated at micellar interface, can form electrical double layer around the micelles. With increasing the surface charge and zeta potential of micelles, increases electrophoretic motion and asymmetric effect.[57-60] Electrical double layers could be either 'Stern layer' and/or 'Gouy-Chapman layer', schemitacally shown in Figure 8.[56, 61-63]

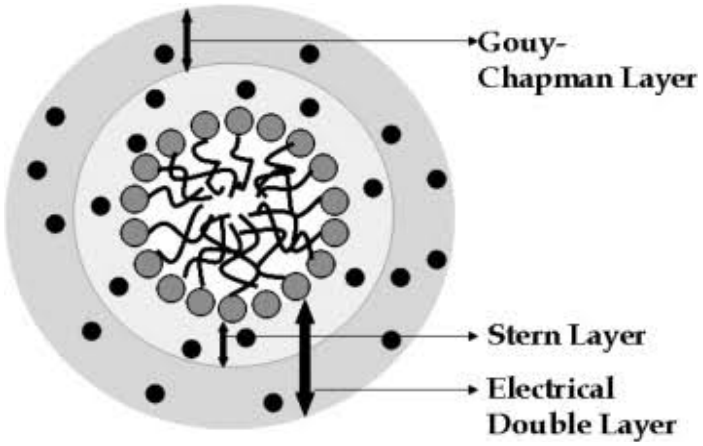

Figure 8. Schematic representation of microstructure of micelle of ionic surfactant. Adopted from Greathouse et al.[56]

5.4. Vesicles. Vesicles are amphiphilic bilayer with spherical geometry. Phospholipid derived vesicles are known as liposomes.[64, 65] Vesicles with a single bilayer are known as unilamellar vesicles while the multilamellar vesicles have more than one bilayers.[66-69] Membrane enclosing vesicles exhibiting similar nature like plasma membrane control the release of contents outside the cell and vice versa.

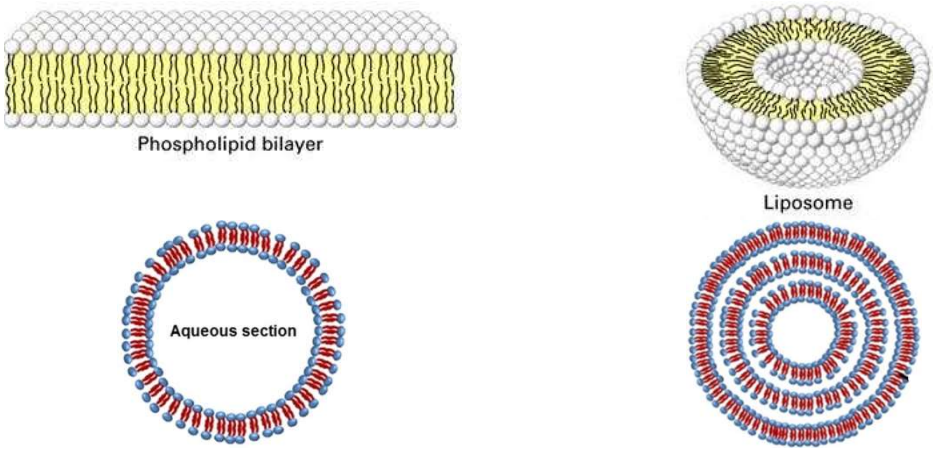

Figure 9. Schematic representation of liposome, phospholipids bilayer, unilamellar and multilamellar vesicle. Adopted from Kaler et al.[70]

Vesicles display versatile applications, *viz.*, drug delivery,[71] nanoparticle synthesis,[72] metabolism[73-75] transport, [72, 73] buoyancy control,[76-78] chemical reaction chambers,[79-81] and enzyme storage.[82-84]

6. *Determination of critical miceller concentration (CMC).*

Most important properties of surfactants are *CMC*. At a fixed environmental condition, different physicochemical techniques of surfactants show remarkable change at the *CMC*, summarized in Figure 10. *CMC* values can be determined by different physicochemical processes, *viz.*, surface tension, conductance, UV-vis absorption/emission spectroscopy.[85]

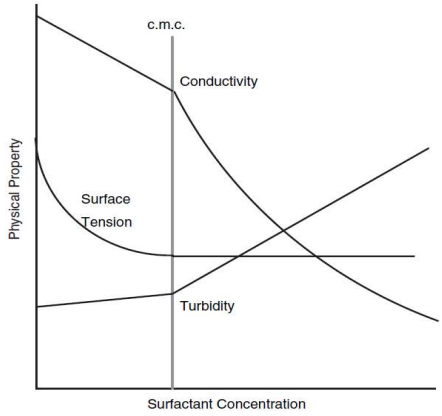

Figure 10. Schematic representation of micelle formation: sudden changes in solution conductivity, irregular variation of surface tension-concentration and rapidly increase in solution turbidity. Adopted from Myers et al.[53]

6.1. Tensiometry. Polar protic solvents exhibit higher surface tension due to the existence of strong intermolecular attractive forces. At lower concentration, surfactant molecules diffuse to air-water interface that subsequently results in an increase in the speacing between the water molecules at the interface. This eventually causes the interfacial tension (γ) to decrease. γ decreases with increasing the concentration of surface active surfactants ([surfactant]) untill the interface becomes saturated, beyond which it attains constancy. Tensiometric profile (γ *vs. log* [surfactant]) shows γ gradually decreases with increasing surfactant concentration, beyond a certain concentration, surface tension values do not change significantly, (Figure 11). The break point refers to *CMC*.

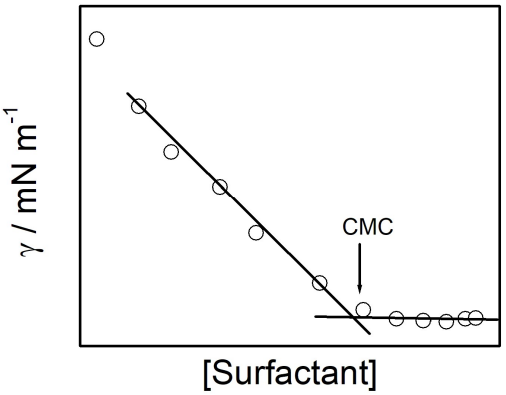

Figure 11. Surface tension (γ) *vs.* surfactant concentration profile of a surfactant solution in water at 298K.

Some important parameters, *viz.*, surface excess (Γ_{max}), minimum molecular area (A_{min}), Gibbs free energy of micellization (ΔG^0_{mic}), surface pressure at *CMC* (π_{CMC}) can be evaluated from the surface tension studies. The maximum surface excess at *CMC* (Γ_{max}) can be evaluated by Gibbs equation:[86, 87]

$$\Gamma_{\max} = -\frac{1}{2.303iRT}\frac{d\gamma}{d\log C} \quad (5)$$

where, C is the molar concentration of the surfactant, '*i*' is the total number of chemical species present in solution per surfactant monomer, R is the universal gas constant and T is the temperature in absolute scale. It is convension to express the $\Gamma_{\max}$ in mole m^{-2}.

The minimum area of the head group at air-water interface ($A_{\min}$, nm^2molecule^{-1}) can be determined using the following equation:[88]

$$A_{\min}(nm^2\text{molecule}^{-1}) = \frac{10^{18}}{N_A\Gamma_{\max}} \quad (6)$$

where, N_A is the avogadro number.

6.2. Conductometry. In this electrochemical method, concentrations of ionic surfactants in water are changed and the conductance values are recorded at 298K. Specific conductance (κ) *vs.* [surfactant] plot for sodium dodecylsulphate is shown in Figure 12.

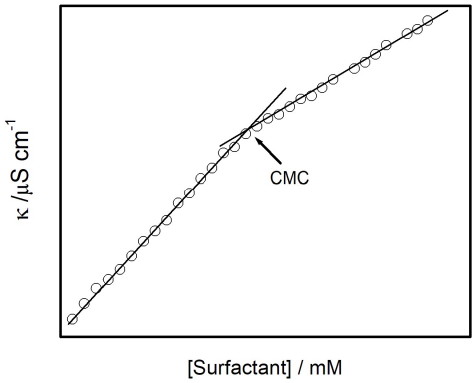

Figure 12. Specific conductance (κ) *vs.* surfactant concentration ([SDS]) plots of a surfactant solution in water at 298K.

With increasing surfactant concentration, κ values sharply increase up to the *CMC*, beyond which conductance increases slowly due to the formation of micelles. The κ *vs.* [surfactant] plot of conductance shows two intersecting straight lines; break point indicates *CMC* of the corresponding surfactant. The fraction of counter ion dissociation (α) can be obtained from the ratio of slope of the post (S_2) and pre (S_1) *CMC* lines.[89] Head group repulsion at micellar surface displays at the 'Stern layer' reduces such repulsive interaction,[90] thus the electrical double layer is formed at the micellar surface. Nature of the ionic surfactants governs the magnitude of α. Degree of counter ion binding (β) thus can be calculated as:[91]

$$\beta = (1 - \alpha) = 1 - \frac{S_2}{S_1} \quad (7)$$

6.3. Absorption spectroscopy. In this approach, a suitable molecular probe is chosen whose spectrum depends on the concentration of surfactant. Pyrene belongs to this category and hence the spectrum of pyrene is recorded in varing surfactant concentration. There exist three major absorption peaks for pyrene at 242, 275 and 338 nm, with four weak bands at 233, 253, 265 and 322 nm respectively. Sum total of the absorbance values of pyrene at its three major peaks are plotted against added surfactant concentrations. Total absorbances (A_T) *vs.* [surfactant] profiles are usually sigmoidal in nature and the *CMC* values are obtained from the midpoint (Figure 13).

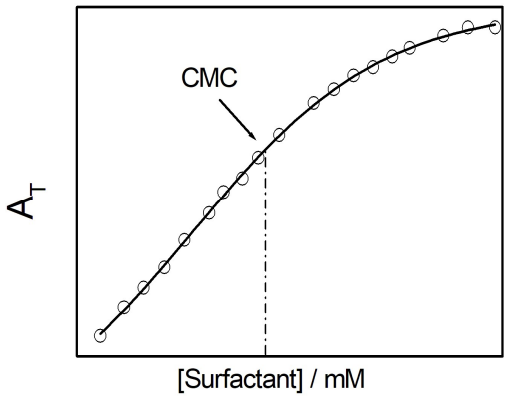

Figure 13. A_T *vs.* surfactant concentration ([surfactant]) profile for pyrene.

The *CMC* value of a surfactant can be calculated by suitabily analyzing the absorption spectra using the following expression:[48]

$$A_T = \frac{(a_i - a_f)}{\left[1+\exp^{\frac{(x-x_0)}{\Delta x}}\right]} + a_f \quad (8)$$

A_T is the sum total absorbance of all major peaks of pyrene, a_i and a_f correspond to the the initial and final asymptotes of the sigmoidal plot respectively. Critical micelle concentration (CMC) value corresponds to the x_0 value (herein the center of the sigmoidal plot, according to the above equation) and Δx is the interval of independent variable x.

6.4. Fluorescence spectroscopy. Critical micelle concentration of surfactants can also be determined by employing fluorescence spectroscopy. As in absorption spectroscopy, surfactant concentration is varied in presence of suitable fluorescent probe; from the profile of fluorescence

intensity *vs.* [surfactant] *CMC* values can be obtained. The method involves the use of a suitable hydrophobic fluorescent probe like pyrene, rhodamine, coumarin and xanthene dyes to the *CMC*.[92-93] Pyrene is a fluorescence probe whose spectrum depends on the polarity of aqueous medium. In aqueous medium, pyrene exhibits five vibronic peaks in the wavelength range 370 to 490 nm. The ratio of first (I_1) at 373 nm and third (I_3) at 393 nm is a marker of solvent polarity. With decreasing polarity of the medium the intensity of third vibronic peak increases significantly compared to the first vibronic peak. As the polarities of a surfactant solution in pre- and post-miceller region are significantly different, hence pyrene fluorescene can be used to determine the *CMC* (Figure 14).

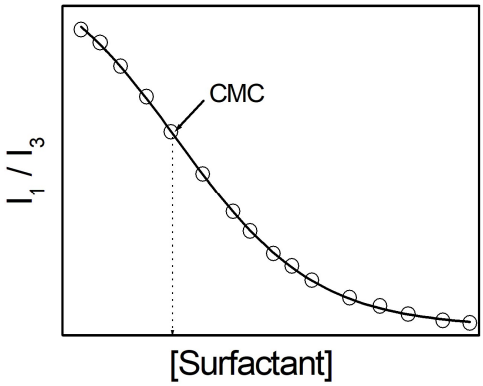

Figure 14. I_1/I_3 *vs.* [Surfactant] profile to determine the *CMC* value of surfactant in water using pyrene as fluorescent probe at 298K.

7. Different models in understanding the micellization processes There are two useful models that help in describing the micellization process: (i) mass action model and (ii) phase seperation model.[94]

7.1. Mass action model. According to this model, above the *CMC*, there exists a dynamic equilibrium between monomer and micelles:[94]

$$nS \overset{K_M}{\Leftrightarrow} S_n \tag{9}$$

where, S and S_n denote surfactant monomer and micelles, n is the aggregation number and micellization constant is represent by K_M. Micellization of ionic surfactants are considered by counter ion condensation and can be defined as:[95]

$$nS^{\pm} + ml^{\pm} \Leftrightarrow (S_n I_m)^{\pm n-m} \tag{10}$$

where, m is the number of counter ion ($I^{\mp}$) associated on per aggregate whereform the equilibrium constant is expressed as:

$$K_{\mathrm{M}} = \left[{(a_M)^{\pm(n-m)}} \Big/ {\{(a_{S^{\pm}})^n (a_{I^{\mp}})^m\}} \right] \approx \left[{(C_M)^{\pm(n-m)}} \Big/ {\{(C_{S^{\pm}})^n (C_{I^{\mp}})^m\}} \right] \quad (11)$$

Gibbs free energy of micellization (ΔG_M^0) can be obtained by using the following equation:[96]

$$\Delta G_M^0 = -\,\mathrm{RT} ln K_{\mathrm{M}} = -\,\mathrm{RT} ln\, (C_M)^{\pm\,(\mathrm{n-m})} + \mathrm{nRT}\; ln\, (C_{S^{\pm}}) + \mathrm{mRT}\; ln\, (C_{I^{\pm}}) \quad (12)$$

$$\Rightarrow \frac{\Delta G_M^0}{n} = -\,\frac{\mathrm{RT}}{\mathrm{n}}\, ln\, (C_{\mathrm{M}})^{\pm(n-m)} + \mathrm{RT}\; ln\, (C_{S^{\pm}}) + \frac{m}{n}\,\mathrm{RT}\; ln\, (C_{I^{\pm}}) \quad (13)$$

As the *CMC* value is significantly small hence and aggregation number (n) is quite large, hence equation 13 can be simplified as:

$$\Delta G_{\mathrm{M}}^0 = \mathrm{RT}\; ln\, (C_{\mathrm{S}^{\pm}}) + \frac{m}{n}\,\mathrm{RT}\; ln\, (C_{\mathrm{I}^{\pm}}) \quad (14)$$

at *CMC*, for an 1:1 ionic surfactant, $C_{S^{\pm}} = C_{I^{\mp}} = CMC$, thus,

$$\Delta G_M^0 = (1+\frac{m}{n})\;\mathrm{RT}\; ln\; CMC = (1+\beta)\;\mathrm{RT}\; ln\; CMC \quad (15)$$

In case of non-ionic surfactants equation 15 gets simplified as:[96]

$$\Delta G_M^0 = \mathrm{RT}\; ln\; CMC \quad (16)$$

In case of mass action model, [96] Gibbs free energy per surfactant monomer (ΔG_{M}^0) can be simplified by taking into account of the contribution of aggregation number:[97]

$$\Delta G_{\mathrm{M}}^0 = (1+\frac{m}{n})\;\mathrm{RT}\; ln\; X_{\mathrm{CMC}} + \frac{\mathrm{RT}}{\mathrm{n}}\, ln\, [2\mathrm{n}\;(\mathrm{n+m})] \quad (17)$$

where, X_{CMC} is *CMC* of the ionic surfactant in mole fraction unit. Enthalpy change (ΔH_{M}^0) of micellization can be obtained by using Gibbs-Helmholtz equation:[97]

$$(\Delta H_{\mathrm{M}}^0)_{\mathrm{vH}} = \left[\frac{\partial (\Delta G_m^0)/T)}{\partial (\frac{1}{T})} \right] = -\mathrm{RT}^2 \left[(1+\frac{m}{n}) \frac{\partial\, ln\, X_{\mathrm{CMC}}}{\partial T} + ln\; X_{\mathrm{CMC}} \frac{\partial (\frac{m}{n})}{\partial T} + ln\; X_{\mathrm{CMC}} \frac{[\partial \left(\frac{1}{n}\right) ln\{2n(n+m)\}]}{\partial T} \right] \quad (18)$$

Last term of Equation 18 can be ignored in case of larger micelles. Thus the above equation can be re-written as:

$$(\Delta H_{\mathrm{M}}^0)_{\mathrm{vH}} = -\,\mathrm{RT}^2 \left[(1+\beta) \frac{\partial ln X_{CMC}}{\partial T} + ln\; X_{CMC} \frac{\partial \beta}{\partial T} \right] \quad (19)$$

For ionic surfactants, change of enthalpy $(\Delta H_M^0)_{\text{cal}}$ values can be determined from the isothermal titration calorimetric studies, using 'van't Hoff' isotherm equation,[98] whereform the associated entropy change of micellization can be defined as:[99]

$$(\Delta S_{\text{m}}^0)_{\text{vH}} = \frac{1}{T}\left[(\Delta H_{\text{M}}^0)_{\text{vH}} - \Delta G_{\text{M}}^0\right] \quad (20)$$

Positive $(\Delta S_m^0)_{\text{vH}}$ values are rarely found.[49]

7.2. Phase separation model. With the help of Phase separation model, above the *CMC* micelles form new phase where micelle and monomer concentration remain invariant. Phase is expressed as:[100]

$$\text{monomer} \Leftrightarrow \text{micelle (pseudo phase)} \quad (21)$$

According to the phase separation model, micelles can form new phase above the *CMC*. The classical thermodynamic formalisms are followed in both the models.

It should be mentioned that both the above mentioned models are not completely prudent to precisely determine the energetices of micellization processess. These two theories are capable to determinie the different thermodynamic parameters of micellization.[101]

8. Miceller aggregation number. Usual number of monomer units per micelle is known as micellar aggregation number (n). It can be determined by fluorescence quenching,[94, 102, 103] static light scattering,[43, 48] small angle neutron scattering[100] and viscometry.[104] Size and shape of the micelles depend on its aggregation number. In case of ionic surfactants 'n' values vary in the range of 20-200 while in case of non-ionic surfcatants, it is usually less than 100.[105] Micellar aggregation number depend on the nature of aggregates,[43,102] counter ion,[102] temperature,[106] pressure,[107] and presence of additives,[43] *etc*. Fluorescence spectra of a fluorescent probe in presence of a surfactant solution ([S] = total surfactant concentration) at different quencher concentration ([Q]) are recorded and the spectra are analyzed in the following way to obtain the aggregation number of micelle (n):[45]

$$ln\,\frac{\text{I}_0}{\text{I}} = \frac{\text{n[Q]}}{\text{[S]}-CMC} \quad (22)$$

where, I_0 and I defines the fluorescence intensity of the fluorescent probe in absence and presence of the quencher used. A plot of $ln\ \frac{I_0}{I}$ *vs.* [Q] has been shown in Figure 15 as representative.

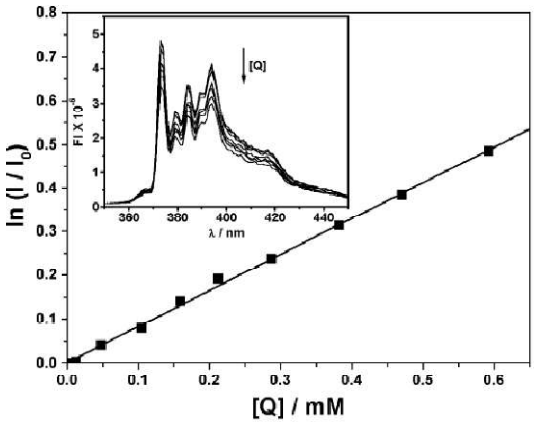

Figure 15. Schematic diagram of *ln* I_0/I *vs.* quencher concentration ([Q]) for pyrene in dodecyltrimethylammonium bromide (C_{12}TAB) at 298K. Inset: Fluorescence spectra of 2 μM pyrene in C_{12}TAB. Hexadecylpyridinium chloride was used as quencher. Adopted from Basu Ray et al.[48]

9. Factors affecting micellization

9.1. Surfactant structure. *CMC* of surfactants depend on size of hydrophilic head and hydrophilic tail of surfactants.

9.1.1. Hydrophilic head group. Hydrophilic head groups influence the aggregation processes. *CMC* values of anionic surfactants are usually lower than their monovalent cationic counter part due to the ionic dissociation and polarity of the hydrophilic groups.[94] Electrostatic interaction between the neighbouring ionic head groups in micelle exhibit unfavourable effect, enhancing *CMC* values.[94,108] *CMC* values of surfactants increased with increasing the hydrophobic interaction between oppositely charge surfactants that follows the sequence: DTAB> SDS > tween-20.

9.1.2. Hydrophobic tail group. In aqueous medium, hydrocarbon chain favours the aggregation processes. With increasing hydrophobicity, *CMC* values gradually decrease.[89, 94] Most experimental data can be fitted as:[109]

$$log\ CMC = \text{A-nB} \tag{23}$$

where, 'n', A and B are the number of carbon atoms in the hydrocarbon chain, and constants for a homologues series, respectively. *CMC* values gradually increase with increasing aqueous solubility of surfactants.[108]

9.1.3. Nature of the counter ion. Counter ions can be affected the micellization process. *CMC* value for cationic surfactants with a particular hydrophobic tail increase in the order: $I^- < Br^- < Cl^- < F^-$. [110] In case of anionic surfactants the order is follow in the order: $Mg^{+2} \sim Ca^{+2} < N^+(CH_2CH_3)_4 < N^+(CH_3)_4 < Cs^+ < K^+ < Na^+$.[43] Surface active ionic surfactants exhibit stronger synergistic interaction with water molecules that corresponds to higher the *CMC*.

9.2. Physical factors. Solvent polarity, temperature, pressure and presence of additives can significantly influence the micellization processes.

9.2.1. Polarity of the solvent. Polar protic solvent is highly favourable for the micellization. The process of micellization gets retarded with decreasing polarity of the medium. Surfactants are oriented at opposite direction of micelle to form reverse micelles.[111, 112]

9.2.2. Temperature. Many physical properties change with varying temperature. Phase behaior of ionic surfactants depend on characteristic temperature. For ionic surfactants usually the *CMC* value increases with increasing temperature that passes through maxima.[113] *CMC* of non-ionic surfactants decrease with increasing the temperature that indicates desolvation of polar head groups.[114]

9.2.3. Pressure. With increasing pressure sterically hindered micelles are formed as well as after the threshold pressure (100-200 Mpa) micellization processes become more spontaneous.[115] With increasing pressure, ionic surfactants corresponds to lower aggregation whereas aggregation numbers of non-ionic surfactants decrease.[116]

9.2.4. Presence of additives. Presences of additives (salt and organic materials) significantly affect self-aggregation process.[90] In dilute solution, added electrolytes reduce the *CMC* of surfactants. For case of ionic surfactants, effect of counter-ion on the *CMC* can be revealed as:[117]

$$log\ CMC = -a\ log\ C_i + b \tag{24}$$

where, ‘a’, ‘b’ and C_i are constants for a given ionic head group and total concentration of monovalent counter ions, respectively. *CMC* values gradually decreases with decreasing the

electrostatic force of repulsions between the oppositely charged head groups. According to Arai,[90,196] *CMC* of non-ionic and zwitterionic surfactants follow the equation:

$$log\ CMC = -\ KC_s + \text{Constant}\ (C_s < 1) \quad (25)$$

where, 'K' is the constant for a particular surfactant, C_s is the concentration of electrolyte.

10. Mixed surfactant systems

It is now a well established fact that mixed surfactant systems exhibit superior behavior than the individual constituent surfactant. Experientally calculated *CMC* values of surfactant mixtures are considerably lower than the theoretically calculated *CMC* that results clearly indicates synergistic interaction between the oppositely charged surfactants. Different physicochemical processes are useed to calculate the *CMC*. Mixed surfactant systems are capable to exhibit superior interfacial adsorption properties due to enhanced hydrophobic interactions between the components.[43, 44, 46, 47, 118] Associative interaction by the oppositely charged surfactants at the bulk and air-water interface are defined using different theoretical models as proposed by Clint, [94, 97] Rubingh, Rosen and Motomura models.[90]

10.1. Clint model. Theoretical *CMC* values for mixed surfactant systems can be predicted by using the Clint equation:[119]

$$\frac{1}{CMC_{\text{cal}}} = \sum_{i=1}^{n} \frac{\alpha_i}{CMC_i} \quad (26)$$

where, α_i and CMC_i is the stoichiometric mole fraction and *CMC* of i^{th} component in the mixture having n number of surfactant components. Clint model can explain the deviation of experimental *CMC* from the theoretical *CMC* values in case of ideal mixing; however, it fails to explain any deviation from ideal mixing (Figure 16).

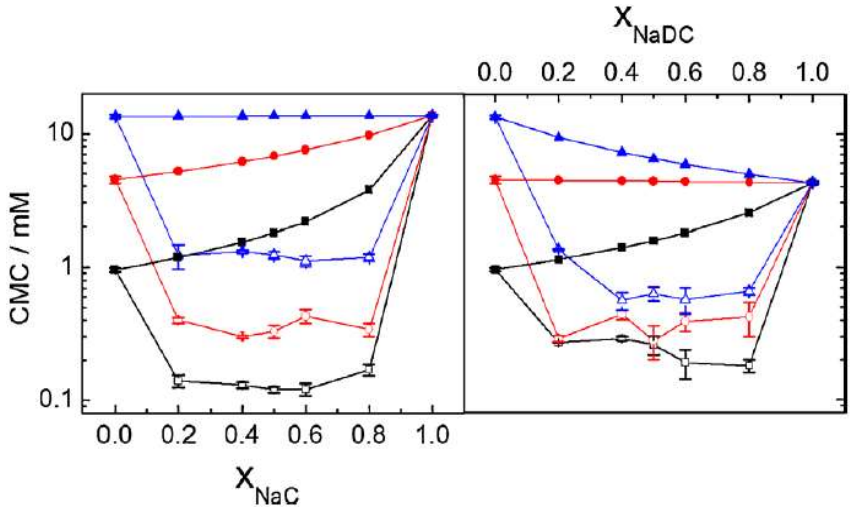

Figure 16. Variation of *CMC* for HTAB+ sodium cholate, NaC (panel A) and HTAB+ sodium deoxycholate, NaDC (panel B) mixed surfactant systems. Open symbols correspond to the experimental values and solid symbols correspond to the theoretically calculated values obtained by Clint equeation. Temperature: 298K. Adopted from Manna et al.[85]

10.2. Rosen model. According to this model, information on the associative interaction among the surfactants in mixed forms are taken into account**.** Rosen et al.[1] could be modify the Clint model with the following propositions: (i) mole fraction of a particular component in the micelle is lower than the overall solution (ii) there occurs synergistic interaction between the components and (iii) increasing hydrophobicity leads to higher synergism. Using standard surface tension data and *CMC* values (experimental and theoretical), activity coefficient of a surfactant in mixed micelle, interaction parameter and micellar composition can be evaluated.

10.3. Rubingh model. Molecular interaction parameters can be calculated in finer way in the light of regular solution theory (RST) proposed by Rubingh.[120] RST helps in micellization process to predict the synergistic interaction between the oppositely charged surfactants. Using Rubingh model one can derive micellar composition and other microstructural parameters.

The afformentioned models will be discussed in subsequent sections or chapters (Chapter 1 and Chapter 2) in detail.

11. Surfactant derived gels.

Apart from micelle, reverse micelle, microemulsion and bilayer, surfactants are also capable to form gels.[121] Physicochemical properties of gels depend on the composition and relative number of alkyl chains per surfactant.[122] Besides, different external parameters, *viz.*, temperature, nature of solvent, pH and additives can also significantly influence the physicochemical properties of gels.

As already been mentioned, stoichimetric mixture of oppositely charged mixed surfactants result in the formation of ion pair amphiphile (IPA). However, if charge density (densities) on the ionic moiety (moieties) of the constuting surfactant(s) is (are) low, then instead of insoluble precipitate, gels are formed. For example when hexadecyltrimethylammonium bromide (HTAB) is stochiometrically mixed with sodium dodecylsulphate (SDS), insoluble ion pair amphiphiles (coacervates) are formed.[123] However, when HTAB is stochiometrically mixed with monosodium salt of *N*-lauroylglycine (C_{12}GlyNa) gels are formed.[124] Besides, gels are also formed with oppositely charged surfactants by judiciously varying the mole ratio (cationic/anionic) as well as the total surfactant concentration.[123] Different types of artificial gels exhibit liquid crystalline behavior. Gels are used in different fields, *viz*., to improve photo optical activity,[125] drug delivery,[126] self-healing materials,[127] biosensors,[128] and hemostasis bandages,[129] to mention a few.

12. Physicochemical characterization of gels. Concentration and composition dependent microstructures of gels can be investigated by different techniques like ternary phase diagram, optical and electron microscopy, scattering studies, thermogravimetric analysis, differential scanning callorimetry and rheology studies.

12.1. Phase manifestation. Truncated phase diagram of cationic/anionic/water system exhibits different types of aggregates like micelle, vesicle, planar bilayer and gel structures.[43, 94]

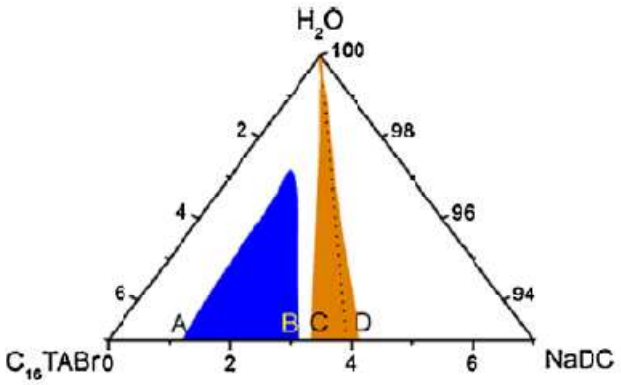

Figure 17. Pseudo ternary phase diagram of hexadecyltrimethylammonium bromide + sodium deoxycholate surfactant mixture at 298K. Adopted from Manna et al.[85]

Composition of different phases can be assessed by analyzing the ratio of the stock solutions of the constituent surfactants. On the basis of visual observation, many samples are prepared at different cationic/anionic (W/W) surfactant ratio and phase boundaries are identified.[130] The different phases are recorded consecutively for a longer time period (at least fifteen days, after which they undergo microbial degradation).

12.2. Microstructural investigation on surfactant gels.

12.2.1. Polarization optical microscopy (POM). POM studies help in identifing different microstructures, liquid crystals and associated textures. Different types of textures like rod and disk like shape,[131] nematic phases,[132] smectic phases and columnar phase,[131] can easily be identified by POM studies. Gels also exhibit flower like,[123] and spherulite,[124] liquid crystal structures (Figure 18).

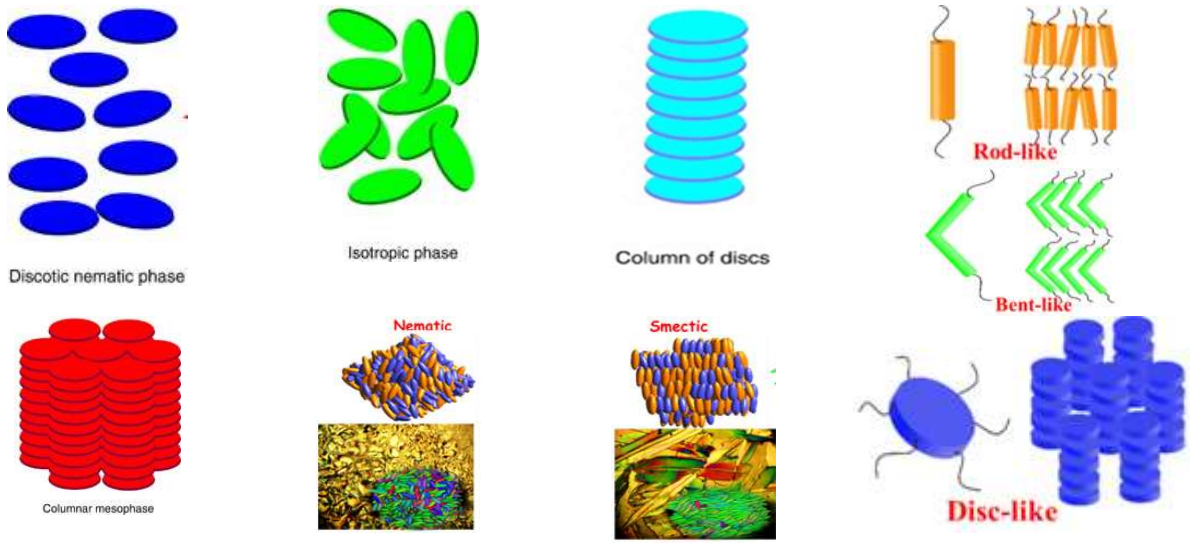

Figure 18. Polarisation optical microscopic images of different liquid crystals.Adopted from Keto et al.[131]

12.2.2. Fluorescence microscopy (FM). Fluorescent dye molecules (both cationic and anionic dyes) are capable to bind to the oppositely charged regions in liquid crystals formed by catanionic surfactant gels. Accordingly, the corresponding fluorescence microscopic images can identify the cation or anion rich regions in liquid crystals, which are observed by POM studies. The cationic dye Rhodamine B exhibits red fluorescence and binds to anionic rich sites. On the other hand, anionic xanthene dye fluorescein shows green fluorescence and interacts with cationic rich region, as shown in Figure 19.

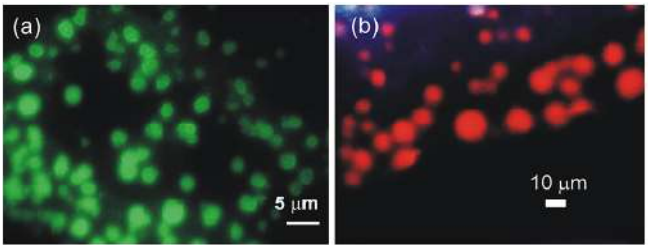

Figure 19. Fluorescence microscopic images of sodium arjunolate in water. System (a) 5, 6-carboxyfluorescien (4.24 x10^{-3} mM) and (b) Rhodamine B (1.73x10^{-3} mM). Adopted from Majumdar et al.[133]

12.2.3. Field emission scanning electron microscopy (FE-SEM). Surface morphology, aggregate size and shape of gels can conveniently be studied by FE-SEM with much higher resolution than optical microscopic studies. The interconnected and fibrous network structure can be identified by such studies.

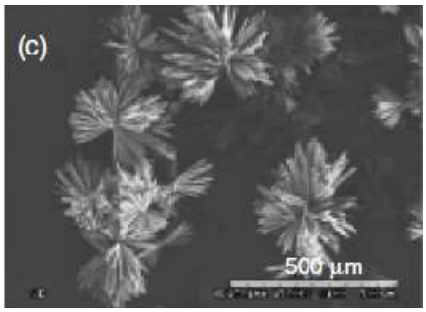

Figure 20. Flower like field emission sanning electron microscopic image of toluene+ethanol mixed gel. Adopted from Caran et al.[134]

12.3. Thermal analysis

12.3.1. Thermo gravimetric analysis (TGA). Phase transition and associated weight loss of surfactant derived gels can be identified by TGA analysis (Figure 21).

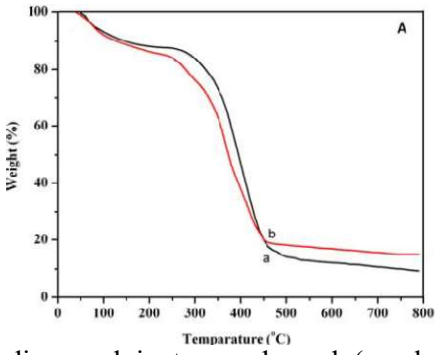

Figure 21. TGA diagram of sodium alginate and poly(acrylamide-*co*-*N*-vinylcaprolactam-*co*-acrylamidoglycolic acid) hydrogels. Adopted from Reddy et al.[135]

TGA profiles quantify the weight loss and thermal stability of gels with varying temperature. It is an especially useful technique in studying gel material, including thermoplastics, thermosets, elastomers, composites, plastic films, fibers, coatings, paints and fuels respectively. Gels show different endothermic peaks in the temperature range 55 to 100°C, due to the dehydration. Systems at further higher temperature undergo chemical decomposition which are identified by the associated weight loss.

12.3.2. Differential scanning calorimetry (DSC). DSC studies are performed in order to understand associated phase transition processes of a material. Different physicochemical parameters, *viz.*, chain melting temperature, width at half peak height of the chain melting temperature, associated enthalpy change and heat capacity changes of surfactant derived gels can be investigated by DSC studies. Peak of the isotherm of aggregates indicate the phase transition and enthalpy change can be evaluated the area of the isotherm.

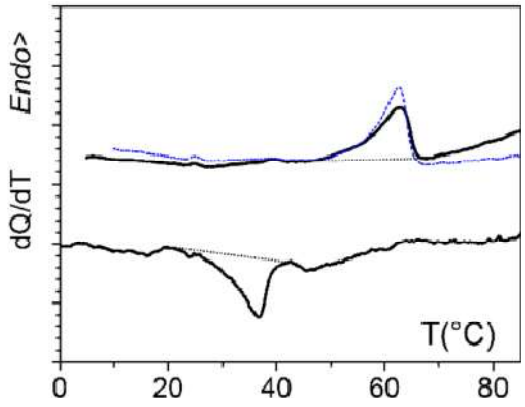

Figure 22. DSC thermogram of oligo phenylenevinylene gels. Adopted from Guenet et al.[136]

12.3.3. Viscosity studies. Viscosity is the resistance of streamline or turbulent flow. Viscosity can be measured by measuring the frictional force, which arises between two adjacent layers of fluid. Usually the viscosities of gels decrease with increasing share rate and increasing temperature (Figure 23).

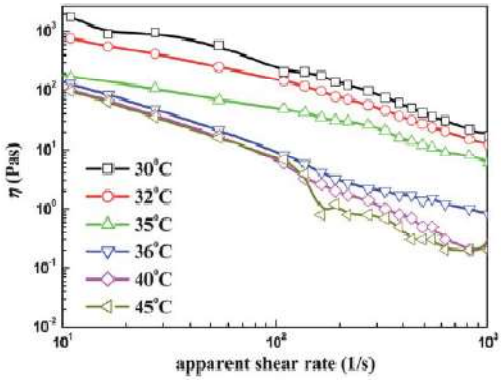

Figure 23. Viscosity of 37.5 wt% gel solution *vs.* apparent shear rate at different temperatures. Adopted from Lu et al.[137]

However some gels do not exert this type of thixotropic behavior. From the rheologial studies it is possible to obtain the response of different materials with the variation of share rate and/or temperature. Suitability of surfactant derived gels are assesed by rheology studies.

13. Application of gels.

Gels have versatile applications in tissue engineering,[138] hemostasis bandages,[139] photo patterning,[140] 3D-printing,[141] electrochemistry,[142] pharmaceutical formulation,[142] and regenerative medicine,[143] *etc*. Recent advances in the design and synthesis of dicarboxylic amino acid based surfactants $(C_{12}AAS)Na_2$ have opened up its wide range of applications as chelator in metal extraction.[124] The considering the "green nature" of $(C_{12}AAS)Na_2$, it is considered to be worthy to investigate the gels formed by it in combination with cationic surfactants. Hexadecyltrimethylammonium bromides (HTAB) combines with $(C_{12}AAS)Na_2$ to form gelatinus aggregates. HTAB exhibits antimicrobial activities however, it shows toxicity. It is therefore believed that when HTAB is combined with $(C_{12}AAS)Na_2$ the individual limitations could be avoided.

14. Metallosurfactants

Functionalizations of complex metal atoms with surfactants are interesting due to its unique properties. Metallosurfactants can form micelle, vesicle, liquid crystal and bilayer at different environmental conditions. Dicarboxylic amino acid based surfactants (C_{12}AAS)Na_2 can interact with bivalent (Ca^{2+}, Mn^{2+} and Cd^{2+}) metal ions, produce water insoluble metallosurfactants, that consist two alkyl chains, considered as pseudo double-tailed amphiphiles. Two alkyl chains associate together due to the strong electrostatic interactions between the two bivalent metal ions and two dicarboxylic amino acids; these complexes exhibits very low solubility in water. Metallosurfactants play crucial rules in forming the bilayer structure.[28,29] Metallosurfactants showed many fold applications in a different industrial fields, *viz.,* recovery of organic complexes, [28] microemulsion, [29] removal of organic pollutants,[144] detergents,[145] microorganism,[146] synthesis of mesoporous materials,[147] *etc*.

15. Physicochemical characterization of metallosurfactants.

Oppositely charged surfactants can be electrostatically interacted with bivalent metals, neutralises the surface charge resulting in the formation of compact ion pair amphiphiles. Precuresors and synthesized metallosurfactants can be characterized by different physicochemical process, *viz.* XRD, NMR and FTIR.

15.1. Structural studies.

15.1.1. XRD studies. Molecular structure and positions of the atoms of metallosurfactant in the crystalline form can be investigated by X-ray crystallography (XRD) studies. XRD studies can find different information, *viz.*, electron density, chemical bonds, crystallographic disorder, salt, metal, mineral, semiconductor, various inorganic, organic biological molecules at the molecular level. Different intensity peaks of precursors and its products can confirm the formation of lamelar structure by the metallosurfactants.

Characteristic XRD pattern of *cis*-chlorobis (ethylenediamine) dodecylaminecobalt (III) nitrate is shown in Figure 24 as representative.

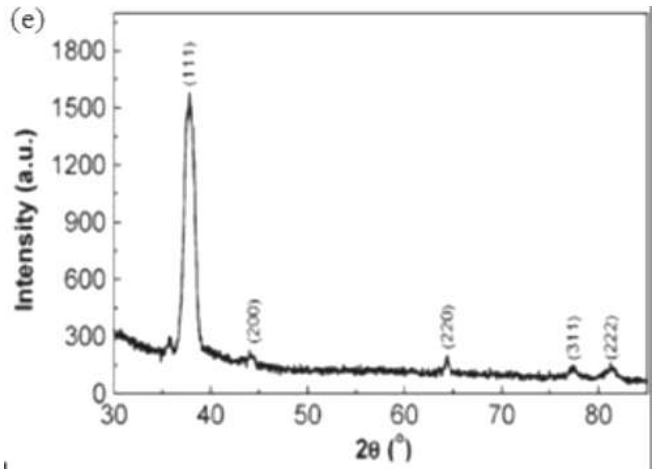

Figure 24. XRD pattern of *cis*-chloro bis (ethylenediamine) dodecylamine cobalt (III) nitrate. Adopted from Garg et al.[148]

15.1.2. Nuclear magnetic resonance (NMR). Formation of metallosurfactants can be investigated by NMR spectroscopic studies. CHN elemental analyses of synthesized element are studied by ^{1}H-NMR spectroscopy and also define symmetrical in nature. Precursors can be distinguished by different types of ^{1}H-NMR protons that varyed with the metallosurfactants. The characteristic intensity peaks of metallosurfactants can be observed due to the interaction between metal ion and surfactant.

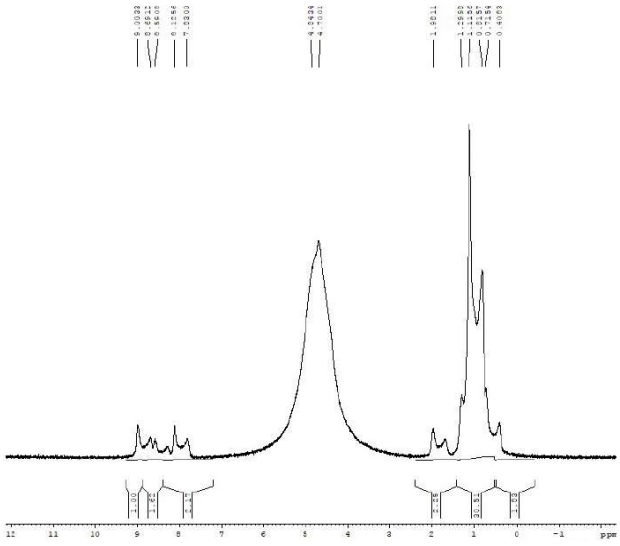

Figure 25. ^{1}H-NMR spectra of bis hexadecyl pyridinium iron (FeCPC II) tetrachloride metallosurfactants. Adopted from Garg et al.[148]

15.1.3. Fourier transformation infrared spectroscopy (FTIR). FTIR spectroscopic studies assign the geometrical configuration of synthesized complexes.

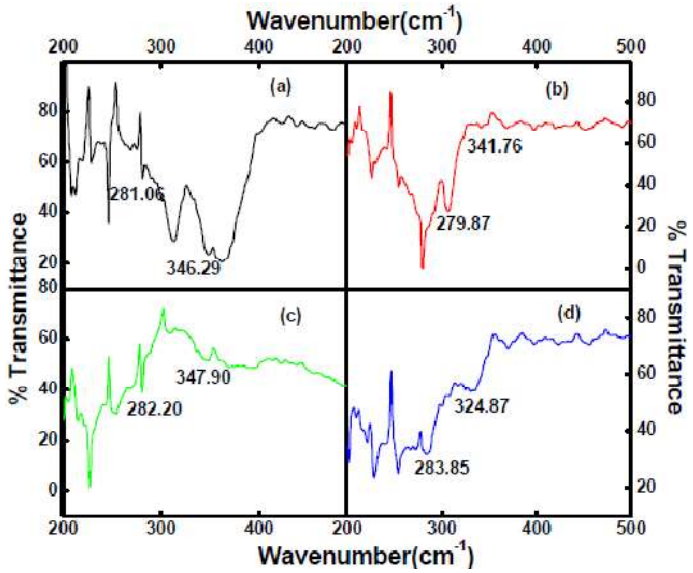

Figure 26. FTIR pattern of bishexadecyl pyridinium iron (FeCPC II) tetrachloride, bishexadecyl pyridinium cobalt (CoCPC II) tetrachloride, bishexadecyl nickel (NiCPC II) pyridinium copper (CoCPC II) tetrachloride metal complexes. Adopted from Garg et al.[148]

Metallosurfactants can display higher stretching frequencies peak than the precursors, due to the higher electrostatic interaction between oppositely charged species. With increasing size of the bivalent metals, electrostatic interaction gradually decreases with opposite charged surfactants, thereby reducing the stretching frequencies. FTIR studies can confirm that metalosurfactants exhibit higher stretching frequencies of different functional groups than its precursors.

15.2. Formation of insoluble monolayer by mettalosurfactants at air-water interface.

Metallosurfactants form insoluble monolayer like other amphiphiles. Thus thay can be studied in combination with phospholipids and cholesterol in the form of monomolecular film to explore their suitability as substitutes of phospholipids in formulating vesicles. Functionality of the metallosurfactants monomolecular flims can be studied by measuring the surface pressure-area isotherm. Structure of the monomolecular flims can be investigated by surface rheology and brewster angle microscopic studies.

15.2.1. Flim functunality studies. Langmuir monolayer is thin layer of soluble organic material, spread over an aqueous surface. Monomolecularfilms of metallosurfactants can be studied by Langmuir surface balance. Upon further compression, incompressible solid phase transitions are noted (Figure 27).

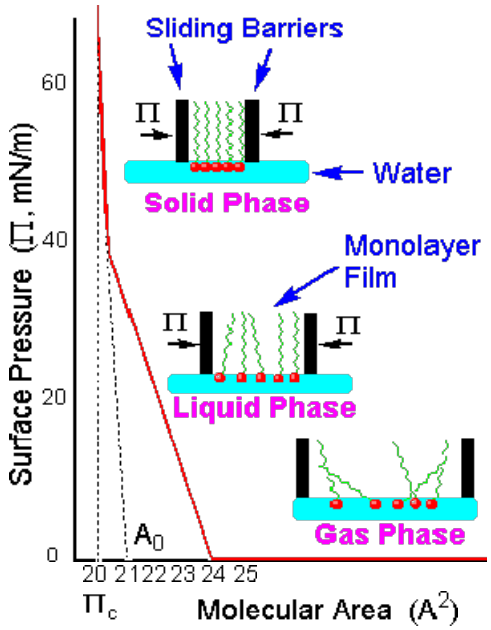

Figure 27. Surface pressure (π)-area (*A*) isotherm of a monomolecular film at air-water interface. Adopted from Shanmugan et al.[149]

Molecules are dispersed on the aqueous surface and loosely pack with water, form gas phase. Gas phase exhibit large molecular area and lower surface pressures. When barriers are brought closer to each other at the same times transition can occur at the air-water interfaces.

Non polar parts of metallosurfactants are protruded away from the solvent while the hydrophilic groups are solvated with water. Surface pressure *vs.* area profile of binuclear azido-bridged complex and thiocyanatobridged are shown in Figure 28.

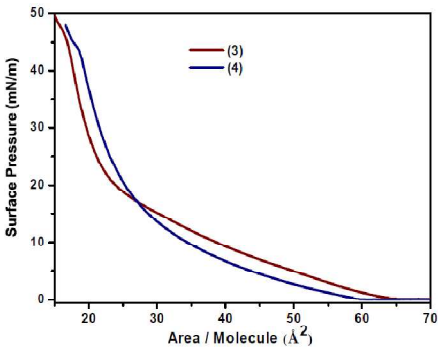

Figure 28. Suraface pressure - area isotherm profiles for binuclear azido-bridged complex and thiocyanatobridged at 298K. Adopted from Shanmugan et al.[149]

Metallosurfactants basically forms expand monolayer, due to the chain mismatch and non spontaneous free energy changes.

15.2.2. Dilatational surface rheology. Interfacial activities of the metallosurfactants monolayer are studied by dilatational surface rheology studies. Surface rheology describes the storage and loss moduli of mixed monolayer.

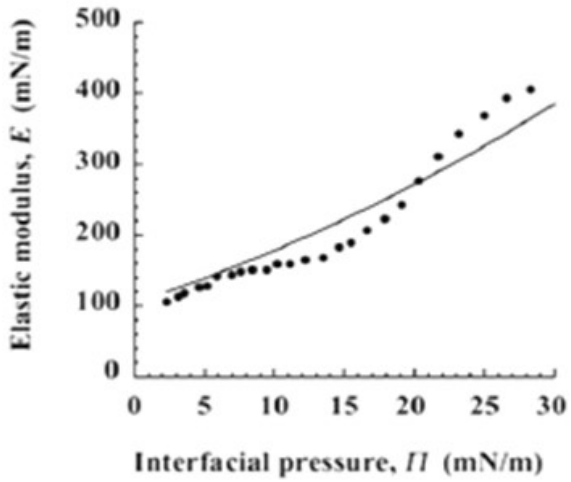

Figure 29. Elastic modulus (E) *vs.* surface pressure (π) plot of cholesterol monolayer. Adopted from Anton et al.[150]

With increasing surface pressure, dynamic surface elasticity of monolayer increase, form relatively rigid spread monolayers. The further increase of π under compression of monolayer leads to a more gradual increase of surface elasticity.

15.3. Structure of the metallosurfactant monolayer.

15.3.1. Brewster angle microscopy (BAM). BAM technique exhibits different mesoscopic structure and texture of mixed monolayers. Polarized light are aimed towards a liquid surface, BAM catches an image when light is reflected from source. Experimental set-up and working principle of BAM is shown in Figure 30. A laser beam is polarized in parallel one dimension plane and directed at the Brewster at (50-55°) angle at air-water interface.

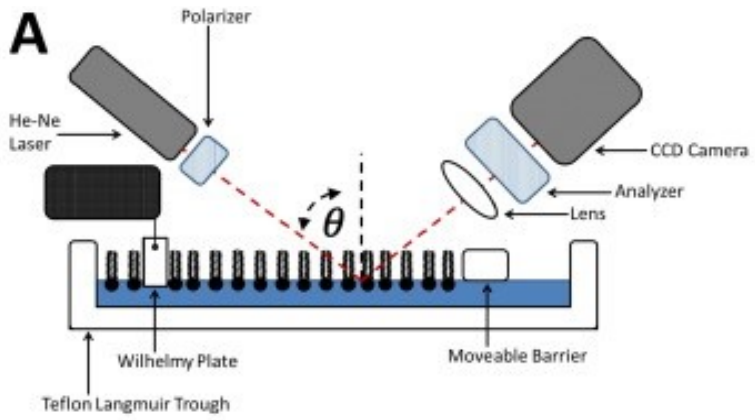

Figure 30. Experimental set up of Brewster angle microscope (A). Adopted from Daear et al.[151]

BAM is connected with Lagmuir surface balance that can provide fundamental information on monomolecular films. Henceforth, monolayers that protrude from the surface and form more ordered regions, display bright images and its can be distinguished qualitative information that is also useful to analyze the phase behavior of the monolayers.

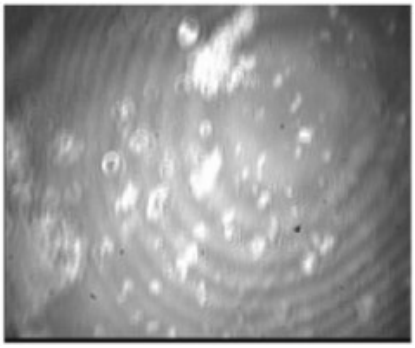

Figure 31. Brewster angle microscopic image of PS0.02 nanoparticles at surface pressures (π) = 10 mN/m. Adopted from Bykov et al.[152]

15.4. Dispersion behavior of metallosurfactants. Metallosurafactants can be dispersed in water to form bilayer, vesicles and micelles. Metallosurfactant combined with phospholipid and cholesterol can form stable hybrid vesicles.

15.4.1. Vesicles formation by metallosurfactants.

Oppositely charged surfactants combined with bivalent metal form stable hybrid vesicles.[15] Size and bilayer thickness of the vesicles depend on charge of counterion and hydrophobic head groups of long chain metallosurfactants. More stable vesicles are formed when the metallosurfactants

are combined with phospholipids and cholesterol. Such, vesicles can be characteritzed using the same techniques and practiced for conventional vesicles.

15.4.2. Characterization of hybride vesicles.

15.4.2.1. Dynamic light scattering (DLS). Solution behaviors of bilayers in the form of vesicles are studied by dynamic light scattering (DLS) studies. The translational diffusion coefficients (D) can be measured by DLS. Hydrodynamic diameter (d_h) of vesicles are determined from following Stocks Einstein equation:[153]

$$d_h = \frac{kT}{3\pi\eta D} \tag{27}$$

where k, T and η indicate Boltzmann constant, temperature and viscosity of water respectively. Hydrodynamic diameter *vs.* time profile of soy phosphatidylcholine+ion pair amphiphile in presence of 30 mole % cholesterol are schematically shown in Figure 32.

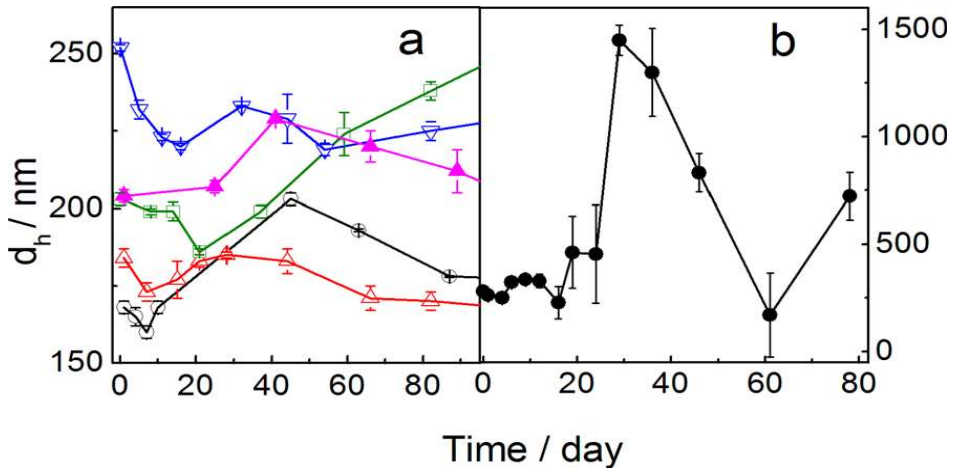

Figure 32. Variation in the hydrodynamic diameter (d_h) *vs.* time profiles for soy phosphotidylcholine (SPC) + ionpair amphiphile (IPA) in presence of 30 mol % cholesterol at 298 K. Concentration of IPA (mol %): Panel a: O, 0; Δ, 10; □, 20; ▽, 30; ▲, 50. Panel b: ●, 40. Adopted from Guha et al.[154]

15.5. Morphological studies.

15.5.1. Transmission electronic microscopy (TEM). In TEM studies a beam of electrons are allowed to transmit through the sample under investigation where the images are obtained according to the contrast of the species. Morphology of vesicles can suitably be investigated by TEM.

Representative image of hybrid vesicles, as shown in Figure 33, can shed light on its size, shape and heterogenity.[155]

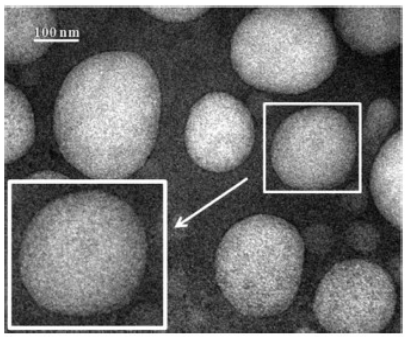

Figure 33. Representative TEM images of soy phosphatidylcholine and ion-pair amphiphile (obtained from and equimolar mixture of sodium dodecylsulphate and hexadecyltrimethylammonium bromide, SPC+IPA 7:3, M/M) vesicles in presence of 30 mole% cholesterol. Adopted from Guha et al.[154]

16. Application of metallosurfactants. Bivalent metallosurfactants exhibit chelating properties, bind with harmful metal and remove through its excretion. Calcium, manganese and cadmium based metallosurfactants form metal chelate complex that can be removed through excretion. Cadmium based metallosurfactants give some information about the solid state and catalytic chemistry as well as manganese containing metallosurfactant can be used as potent sensitizing agents, capable to inducing hypersensitivity due to the structural stabilities. Metallosurfactants display versatile application, *viz*., drug delivery, encapsulation, microreactors and model membrane, drug encapsulation, antibacterial formulation and nanomaterial synthesis. Keeping in mind the aforementioned perspectives, the present dissertation endeavoers to undertake physicochemical investigations on dicarboxylic aminoacid based surfactants in combination with hexadecyltrimethylammonium bromide in the form of adsorb monolayer, micelle and gels. Also, the metallosurfactants are prepared by $(C_{12}AAS)Na_2$ combination with bivalent metals, *viz.,* Ca^{2+}, Mn^{2+} and Cd^{2+}. Metallosurfactants were studied in combination with soy phosphatidylcholine and cholesterol in the form of solvent spred monolayer and hybrid vesicles. Biocompatibilities of the systems were also investigated with the intention to use them as alternative carriers for drugs. It is believed that interfacial and aggregation behaviors of surfactant mixtures have been provided new insights, which will eventually help in understanding the formation of hybrid vesicles.